CLINICAL-DIAGNOSTIC STUDIES

A PILOT SHOTGUN PROTEOMIC PROFILING OF PERIPHERAL BLOOD MONONUCLEAR CELLS IN PATIENTS WITH DIFFERENT MRI PHENOTYPES OF CEREBRAL SMALL VESSEL DISEASE

A.A. Geints[1]*, P.S. Shlapakova[1], L.A. Dobrynina[1], E.I. Kremneva[1], E.V. Khriapova[2], V.G. Zgoda[2], O.V. Tikhonova[2]

[1]Russian Center of Neurology and Neurosciences,
80 Volokolamskoye shosse, Moscow, 125367 Russia; *e-mail: gejnts.a.a@neurology.ru
[2]Institute of Biomedical Chemistry, 10 Pogodinskaya str., Moscow, 119121 Russia

Age-related cerebral microangiopathy (CMA) also known as cerebral small vessel disease (CSVD), is a leading cause of cognitive impairment and stroke. Difficulties in studying CSVD are associated with limitations in visualizing small vessels and diagnostics based on MRI signs of brain damage (white matter hyperintensity, lacunae, microbleeds, etc.). Our previous assessment of each CSVD MRI feature using a four-point severity scale and distribution among brain region using cluster analysis revealed the existence of two MRI types. They do not differ in the severity of vascular risk factors but do differ in the severity of clinical manifestations and levels of circulating plasma biomarkers. Here we present results of a pilot panoramic study of the proteome of peripheral blood mononuclear cells from patients with CSVD MRI types I and II, as well as healthy volunteers. CSVD patients showed a tendency toward downregulation of proteins associated with vesicular trafficking and extracellular matrix (ECM) remodeling relative to control values. Patients with CSVD MRI type 1 showed trends toward insufficient activation of protective proteins (arginase-1, thioredoxin, autophagy and protein stress regulators) and excessive activation of platelet proteins and vascular wall remodeling regulators (such as profilin-1), compared to patients with CSVD MRI type 2. These results indicate the need to study the microstructure of the basement membrane, vascular ECM, and perivascular spaces in cerebral small vessels.

Keywords: cerebral microangiopathy; cerebral small vessel disease; proteomic studies; magnetic resonance imaging; STRIVE criteria; protein mass spectrometry

DOI: 10.18097/PBMCR1643

INTRODUCTION

Cerebral microangiopathy (CMA) also known as cerebral small vessel disease (CSVD) is the cause of more than 25% of ischemic strokes, the majority of spontaneous intracerebral hemorrhages, up to 45% of dementia cases, as well as gait disturbances and emotional disorders in older and elderly people [1–6].

The development of CSVD is associated with damage to small vessels of the brain — perforating arterioles, venules, and capillaries involved in the formation of the neurovascular unit (NVU) and the blood-brain barrier (BBB). Classical concepts of CSVD are based on the leading pathogenetic role of arterial hypertension (AH), causing arteriolosclerosis and cerebral ischemia [7–13]. However, therapeutic strategies aimed at AH control have shown questionable benefits in delaying brain damage in CSVD [12]. There is an increasing number of cases of CSVD without AH and mixed forms with neurodegeneration [14–17].

In 2013, the STRIVE (STandards for Reporting Vascular Changes on Neuroimaging) diagnostic MRI criteria were proposed. These criteria correspond to the main pathological features of small vessel damage in the brain in CSVD (WMH, small subcortical infarcts, lacunae, dilated perivascular spaces, cerebral microbleeds, and cerebral atrophy) [2]. The STRIVE criteria opened the possibility of prospective studies of CSVD at the population level, but did not demonstrate a correlation with the severity of clinical manifestations [18].

Abbreviations used: AH – arterial hypertension; ARSA – arylsulfatase A; BBB – blood-brain barrier; CMA – cerebral microangiopathy; CSVD – cerebral small vessel disease; ECM – extracellular matrix; GALNS – N-acetylgalactosamine-6-sulfatase; IGJ – immunoglobulin J chain; LFQ – label-free quantification; LRG1 – leucine-rich alpha-2-glycoprotein; NVU – neurovascular unit; SORL1 – sortilin-related receptor; SYTL4 – synaptotagmin-like protein 4; TIMP2 – inhibitor of metalloproteinases 2; TXN – thioredoxin; WMH – white matter hyperintensity.

© 2026 by the authors. Licensee IBMC, Moscow, Russia. This article is an open access and distributed under the terms and conditions of the Creative Commons Attribution (CC BY-SA 4.0) license (http://creativecommons.org/licenses/by-sa/4.0/).

These observations prompted the scientific community to continue studying the CSVD pathogenesis by means of modern molecular genetic methods. Over the past decade, population studies of genetic polymorphisms and gene expression patterns were conducted for most STRIVE criteria [19]. The functions of at least 15 genes associated with hereditary forms of CSVD (up to 5% of cases) have been studied in details [20]. Highly significant evidence exists for the importance of non-ischemic mechanisms associated with impaired NVU functioning in the development of CSVD: endothelial dysfunction, increased permeability of the BBB, neuroinflammation, glymphatic dysfunction and neurodegeneration, changes in the molecular composition and architecture of the ECM [21, 22]. These processes are also actively involved in the development of cognitive disorders [6, 23, 24]. However, clarified pathogenetic mechanisms have not culminated in the development of pathogenetic therapy for CSVD [25].

Multi-omics technologies, such as massively parallel nucleic acid sequencing and protein mass spectrometry, are used to study age-related CSVD to a significantly lesser extent than for neurodegenerative and cardiovascular diseases. Single-cell RNA sequencing has revealed a unique population of endothelial cells with a premature aging phenotype in patients with advanced CSVD, both in the affected and unaffected white matter [26]. A correlation has been established between the volume of WMH and the rate of biological aging, calculated from the methylation profile of CpG islands in the genome [27, 28].

Proteomic studies of CSVD still represent a rather rare event. Plasma protein profiling in over 800 patients with CSVD revealed altered expression of proteins, mainly possessing peptidase activity, localized in the ECM or vesicles involved in inflammation, hemostasis, transport and metabolism of IGF-signaling components, and ECM organization [29, 30]. A proteomic study of cerebrospinal fluid in over 80 patients with various MRI features of CSVD (WMH, lacunae, microbleeds) revealed a significant association of WMH with increased levels of matrix metalloproteinases (in particular, MMP12), elastin, and collagen proteins in the cerebrospinal fluid even at early stages of CSVD [31].

There are a number of limitations that hinder effective development of experimental pathogenetic therapy for CSVD. Molecular genetic study designs are limited in their effectiveness and reproducibility due to the lack of standard approaches for comparing the obtained data with the quantitative and spatial distribution of combined MRI features of CSVD, especially in the late stages of the disease. However, recent population studies have noted that a multiple increase in the number of significant genetic polymorphisms is detected when MRI features of CSVD are subdivided by location, for example, into deep and periventricular WMH [32], lobar and deep MCI [33], and dilated perivascular spaces in the white matter and basal ganglia [34].

We previously classified CSVD forms based on their distribution across brain regions and severity according to a four-point scale of their MRI features [35]. In a sample of nearly 100 cases of advanced CSVD characterized by widespread confluent WMH (Fazekas stage 3), the MRI data of the patients were divided into MRI type 1 and MRI type 2 based on hierarchical agglomerative cluster analysis and an iterative k-means algorithm [35]. The two variants insignificantly differed in the representation and severity of vascular factors. We have demonstrated that MRI type 1 is characterized by more pronounced periventricular WMH, multiple lacunae and microbleeds, cerebral cortex atrophy, as well as a more severe spectrum of clinical manifestations (pronounced cognitive impairment and gait disturbances) and younger age. In MRI type 2, hyperintensity of the deep and juxtacortical white matter was combined with isolated lacunae without microbleeds or cortical atrophy, as well as milder clinical manifestations, and was older. Based on ELISA studies of blood plasma parameters associated with damage to the vascular wall and brain, as well as MRI studies of pathophysiological mechanisms — BBB permeability using T1-dynamic contrast, pulsatility of blood vessels, and the ratio of brain hydromedia (venous and arterial blood flow and cerebrospinal fluid flow), it has been elucidated that ischemia and depletion of angiogenesis play a dominant role in the formation of MRI type 1, while in MRI type 2, the main pathogenetic factor is impaired BBB permeability and chronic inflammation [35].

Multimodal validation of this subdivision of advanced CSVD stages into MRI types involves searching for differentiating molecular genetic signatures. This article presents the results of a pilot study aimed at elucidation of associations between the protein expression profile of peripheral blood mononuclear cells and two main MRI types of age-related CSVD.

MATERIALS AND METHODS

Sample Set Description

The study included six CSVD patients (3 men and 3 women, aged 64±8.8 years) and three healthy volunteers (1 man and 2 women, aged 64±8.5 years). MRI examinations were performed using a 3T magnetic resonance imaging (MRI) scanner (Siemens Healthineers AG, Germany).

MRI features of CSVD were assessed, while other MRI abnormalities were excluded. All CSVD patients had MRI features that met the STRIVE criteria and were pronounced (Fazekas stage 3 WMH, lacunae, and microbleeds). According to our developed method for determining MRI types of CSVD [32], three CSVD patients were classified as MRI type 1 (2 men and 1 woman, aged 64±9.6 years), and three patients as MRI type 2 (1 man and 2 women, aged 65±10.0 years). No pathological MR signs were observed in healthy volunteers. The exclusion criteria for the study were: history of subcortical infarction within the last 3 months, history of hemorrhagic or ischemic stroke (not lacunar); cardiac pathology with a reduced ejection fraction < 50%, atherosclerotic stenosis of the brachiocephalic arteries > 50%, chronic kidney disease with GFR < 30 ml/min, decompensated type 2 diabetes mellitus, thyroid dysfunction without euthyroidism, cancer, previous infectious or acute somatic illness, or surgery within the last month.

Sample Preparation

Blood was collected in the morning on an empty stomach into EDTA vacutainers. The resulting samples were stored at 4°C for no more than 5 h. Leukocytes were isolated from 400 μl of fresh peripheral blood after two washes with cold water without RNases and two washes with cold PBS (centrifugation for 3 min at 500 *g*). The cell pellet was stored in a buffer containing 2% SDS in 100 mM triethylammonium bicarbonate (TEAB, Fluka Analytical, Switzerland), pH 8.5, at -20°C.

After thawing, 50 μl of a solution containing 10% SDS in 100 mM triethylammonium bicarbonate buffer (TEAB, Fluka Analytical) were added to each sample to a final concentration of 5% SDS and 50 mM TEAB (pH 8.5). The resulting solutions were processed using a Bandelin Sonopuls ultrasonic homogenizer (Bandelin Electronic GmbH & Co., Germany) (30% power) for 30 s on ice and then the samples were centrifuged at 10,000 *g* for 3 min at 4°C.

For hydrolytic cleavage of proteins with trypsin (Promega, USA), S-trap spin columns (Protifi, USA) were used in accordance with the manufacturer's recommendations, as described previously [36]. The resulting supernatant (tryptic digest) was dried in a Concentrator 5301 vacuum concentrator (Eppendorf, Germany). Peptide concentrations were determined colorimetrically using a Pierce Quantitative Colorimetric Peptide Assay kit (Pierce, USA) in accordance with the manufacturer's recommendations. The peptides were then dried, dissolved in 0.1% formic acid to a concentration of 1 μg/μl, and submitted for proteomic analysis.

Shotgun Mass Spectrometry (MS) Analysis

The resulting hydrolysates were analyzed in triplicates for each sample using an Ultimate 3000 RSLC-nano UHPLC system (Thermo Scientific, USA) coupled to a Q Exactive HF-X Quadrupole-Orbitrap high-resolution mass spectrometer (Thermo Scientific). Samples were loaded in equal amounts (2 μl each) onto an Acclaim μ-Precolumn enrichment column (0.5 mm × 3 mm, 5 μm particle diameter) (Thermo Scientific) and washed with mobile phase C (2% acetonitrile, 0.1% formic acid in deionized water) at a flow rate of 10 μl/min for 4 min in isocratic mode. The peptides were then separated on a PeakyEfficiency HPLC column (FE 100 μm × 30 cm, 1.9 μm particle size) (Molekta, Russia) in gradient elution mode. The gradient was formed using mobile phase A (0.1% formic acid) and mobile phase B (80% acetonitrile, 0.1% aqueous formic acid) at a flow rate of 0.3 μl/min. The column was washed with 2% mobile phase B for 4 min, and then the concentration of mobile phase B was linearly increased to 35% over 74 min, then the concentration of phase B was linearly increased to 99% over 2 min, after 5 min of washing with 99% buffer B, the concentration of this buffer was linearly decreased to the initial 2% over 3 min. The total duration of the analysis was 90 min.

MS analysis was performed in positive ionization mode using a NESI source (Thermo Scientific). The following parameters were set for the MS analysis: emitter voltage of 2.1 kV, capillary temperature of 240°C. Panoramic scanning was performed in the mass range from 450 *m/z* to 1500 *m/z*, at a resolution of 60,000. For tandem scanning, the resolution was set to 15,000 in the mass range from 100 *m/z* to the upper limit, which was determined automatically based on the precursor mass. Precursor ion isolation was performed in a window of ±1 Da. The maximum number of ions allowed for isolation in MS2 mode was set to 20, with a precursor cutoff for tandem analysis of 500,000 units and a normalized collision energy (NCE) of 29. Only ions with charge states between $z = 2+$ and $z = 6+$ were considered for tandem scanning. The maximum accumulation time for precursor ions was 50 ms, and for fragment ions, 110 ms. The AGC values for precursors and fragment ions were set to 1×10^6 and 2×10^5, respectively. All measured precursors were dynamically excluded from tandem MS/MS analysis for 90 s. A commercially available cytochrome *c* digest (Dionex™ Cytochrome C Digest, Thermo Scientific) was used for quality control of the MS analysis.

Protein Identification and Shotgun Proteomic Data Analysis

For nine samples, MaxQuant software (version 2.0.3.0, Max Planck Institute of Biochemistry,

Germany) with the built-in Andromeda algorithm [37] was used to identify proteins and calculate the LFQ index for their quantification. The FASTA file containing amino acid sequences of human proteins (proteome UP000005640, 15.05.2023) and its inverted analog were used to calculate the false-positive rate (FDR). The following search parameters were set for protein identification: trypsin as the cleavage enzyme, monoisotopic peptide mass determination accuracy of ±4.5 ppm, MS/MS mass determination accuracy of ±20 ppm, and one missed trypsin cleavage site. Methionine oxidation, N-terminal acetylation, and cysteine carbamidomethylation were considered as possible and a fixed peptide modification, respectively. The "matching between runs" (MBR) option was enabled with default parameters. To validate Peptide-Spectrum Matches (PSM) spectra and peptide pairings and to identify peptides and proteins, an FDR of 0.01 was used as a threshold.

For further statistical analysis, LFQIntensity values for proteins in all samples (including technical replicates), were loaded from the MaxQuant "proteinGroups.txt" output file into Perseus 2.1.3.0 (Max Planck Institute of Biochemistry) [35]. The data were pre-filtered: common protein contaminants and false-positive identifications were removed, and proteins identified by two or more peptides were retained in the analysis. For quantitative analysis of protein content in nine samples, log2-transformed LFQ values, normalized by Z-score and filtered by seven valid LFQ values out of nine, taking into account technical replicates for at least one study group, were used. After hierarchical clustering with default parameters, three samples with significantly different protein profiles were removed from the analysis due to contamination of leukocyte cells with major human blood proteins.

For the development of an alternative approach of assessing contamination of selected six samples (two patients with MRI type 1, two patients with MRI type 2, and two healthy volunteers) with blood components, the R/Bioconductor software (MSnSet.utils package) was used. Major blood proteins (hemoglobin, fibrinogen, albumin, spectrin) were searched using protein identifiers in MSnSet (using NCBI RefSeq protein IDs). Based on the calculated LFQ scores, a logical vector was created to calculate the average "presence" value of the identified proteins in the samples, followed by a density plot (KDE plot). In further analysis, the listed contaminant proteins in the remaining six samples were ignored.

For quantitative analysis of protein content in the samples, log2-transformed LFQ values, normalized by Z-score and filtered by valid LFQ values (5 valid values out of 6 in at least one experimental group) were used. Missing LFQ values in each sample were supplemented by sampling values from a normal distribution with a width (spread) of 0.5 sigma from the actual standard deviation of the sample and a standard deviation reduction of 1.4 sigma. Differential protein expression was assessed between cohorts (CSVD vs. normal, MRI type 1 vs. normal, MRI type 2 vs. normal, MRI type 1 vs. MRI type 2) using the Student's *t*-test (q-value < 0.05, s0 = 1) with the default permutation-based FDR adjustment provided by the software. The resulting differential expression analysis data were visualized using Volcano-plot. Differences in protein content were considered as statistically significant at a q-value < 0.05 and a fold change FC > 2 (i.e., $\log_2 FC > 1$).

To construct a heat map of protein expression profiles, a preliminary comparison of three cohorts (MRI type 1, MRI type 2, normal) was performed using ANOVA, followed by pairwise comparisons using Tukey's post-hoc HSD test (q-value < 0.05). For all proteins with statistically significant expression changes identified by this method, hierarchical clustering of samples by expression profile similarity was performed using the k-means method (K = 20). Functional annotation of proteins with significantly altered expression was performed using the Fisher's exact method based on international molecular pathway databases (GO, GSEA, Reactome, KEGG, Pfam, interpro) [38]. Protein-protein interaction analysis was performed using the STRING program [39].

RESULTS

After removing common contaminants and false-positive identifications, shotgun proteomic analysis reliably detected 1,554 proteins in nine samples. Sample quality control performed using hierarchical clustering revealed significantly different protein profiles in three samples: the three experimental groups the number of identified proteins with valid LFQ values reduced by almost threefold (574 proteins). This may be due to contamination of the isolated leukocyte samples with major blood proteins and can reflect the problem dynamic concentration range of blood proteins influencing results of proteomic analysis of this biological material. Six samples characterized by more representative protein profiles out of 703 proteins were selected for further analysis, and additional contamination with non-target blood components was assessed for these samples.

Sample Contamination Assessment

For six samples, an additional search for major blood proteins (hemoglobin, fibrinogen, albumin, spectrin) was performed, creating a logical vector for calculation of the average "presence" value of the identified proteins in the samples, followed by plotting a density plot (KDE-plot) (Fig. 1A).

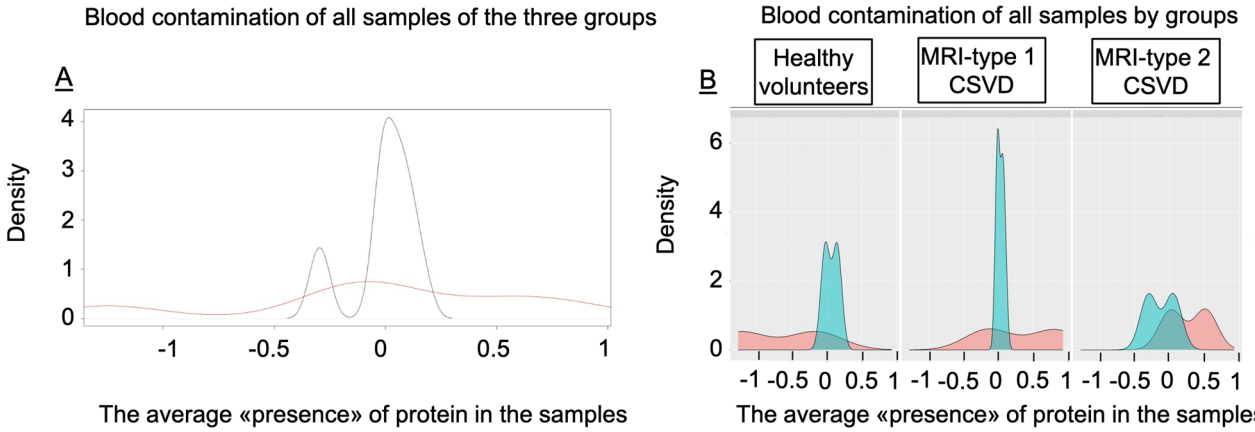

Figure 1. Visualization of blood component contamination (KDE plot). **A** – Blood contamination of all studied samples: red line – contaminating proteins, black line – proteins of interest. **B** – Blood contamination of samples of individual groups. The area under the curve highlighted in red shows contaminating proteins and the area under the curve highlighted in blue shows proteins of interest. The color version of the figure is available in the electronic version of the article.

Both MRI type 2 samples demonstrated significant contamination with non-target blood components (Fig. 1B), thus demonstrating one of the limitations of this pilot study.

Assessment of Differential Expression of Protein Groups

After the initial processing of MS data, 703 protein groups were used for statistical analysis (Supplementary Materials, Table S1). Descriptive statistics (mean, median, standard deviation, and range) are presented in the Supplementary Materials (Supplementary Materials, Table S2). For the four CSVD patients we found a significant decrease in the expression of 141 proteins and an increase in the expression of 92 proteins (q-value < 0.05, s0 = 1) (Fig. 2A; Supplementary Materials, Table S3) as compared to two healthy volunteers. The most pronounced decrease in expression was observed for proteins involved in ECM remodeling (TIMP2, GALNS, ARSA) and modulation of TGFβ signaling (LRG1). The most significantly increased expression was demonstrated by immunomodulatory proteins (IGJ, CD5-like protein (CD5L)), as well as regulators of epithelial barrier integrity and transcellular trafficking (Ras-family protein Rab-10, moesin (MSN)).

Additionally, the differential expression of protein groups was assessed for patients with two different CSVD MRI types. During comparison of the cohort of patients with MRI type 1 relative to healthy volunteers, we identified a significant decrease in the expression of 136 proteins and an increase in the expression of 217 proteins (q-value < 0.05, s0 = 1) (Fig. 2B; Supplementary Materials, Table S3). The most pronounced decrease in expression was found in the case of the aforementioned GALNS, immunomodulatory proteins of eosinophil granules (eosinophil basic protein (RNASE3), eosinophil neurotoxin (RNASE2), eosinophil peroxidase (EPX)), and inflammation-associated proteins (CLEC5A lectin, CR1 complement receptor). The proteins with the most significant increase in expression differ in function, but all are potentially involved in the regulation of BBB integrity through intercellular adhesion and transcellular trafficking — IGJ, SYTL4, phosphatidate cytidyltransferase 2 (CDS2), myosin regulatory light chains (MYL12A/B), and alpha-4 tropomyosin chain (TMP4) [41–45].

In a cohort of CSVD patients with MRI type 2, we found a significant decrease in the expression of 143 proteins and an increase in the expression of 88 proteins (q-value < 0.05, s0 = 1) (Fig. 2C; Supplementary Materials, Table S3) as compared to healthy volunteers. The most pronounced decrease in expression was again observed for proteins indirectly affecting ECM remodeling: ARSA, LRG1, SORL1, and TIMP2. The most pronounced increase in expression was obtained for proinflammatory complement proteins (CFB, CFH), immunoglobulin chains (gamma and lambda), and vasomodulators (arginase-1, histidine-rich glycoprotein HRG). However, taking into consideration the presence of contamination of this type of samples with non-target blood proteins, these changes can be considered nonspecific and further study is clearly needed.

For the cohort of patients with MRI type 1, relative to the cohort of patients with MRI type 2, we found a significant decrease in the expression of 27 and an increase in the expression of 152 proteins (q-value < 0.05, s0 = 1) (Fig. 2D; Supplementary Materials, Table S3). The greatest reduction in protein expression was found in the case of protective stress proteins: arginase-1, a modulator of vascular tone, Ral-A, a regulator of vesicular trafficking and

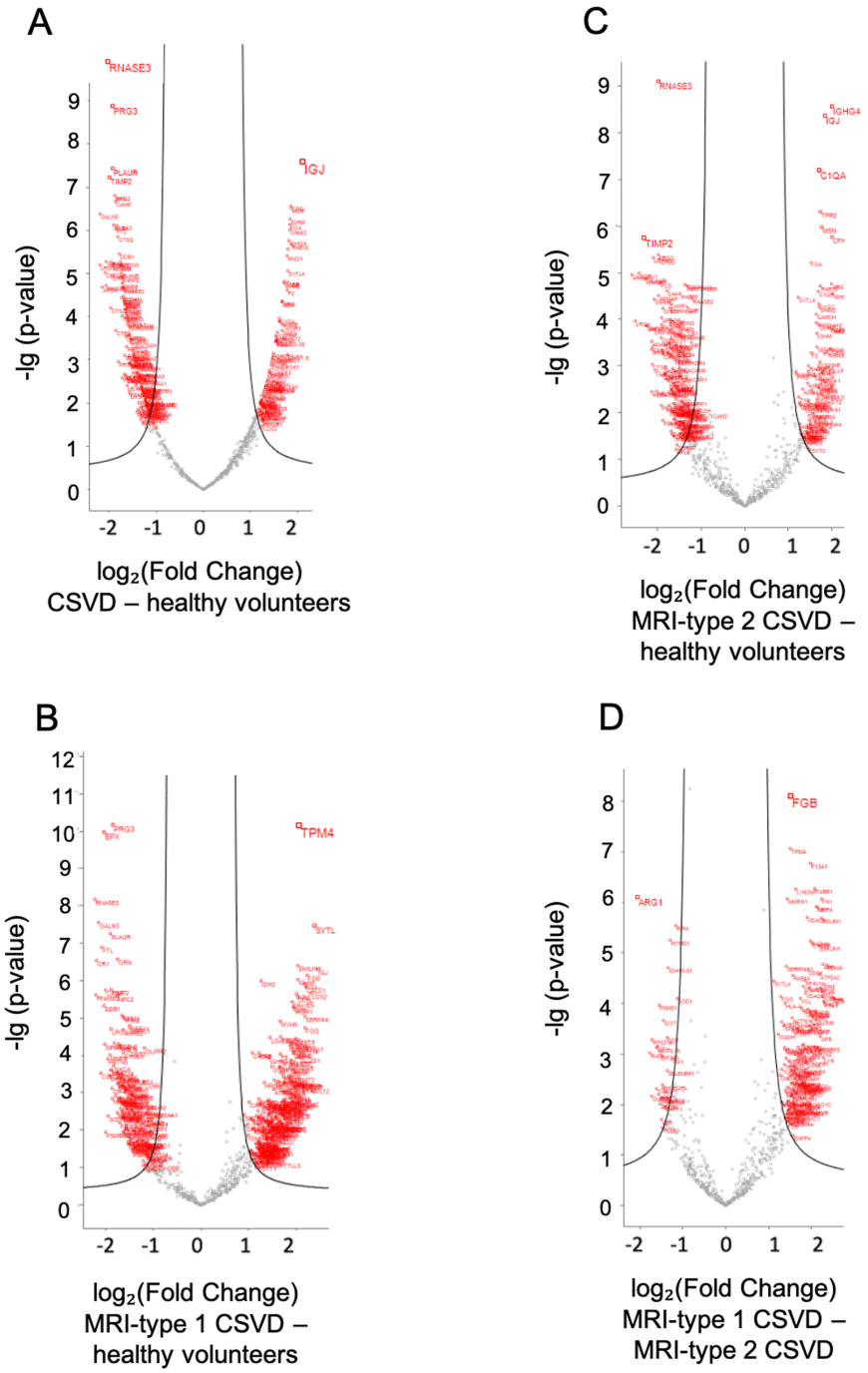

Figure 2. Volcano-plot graphs showing differential protein expression (log2(Fold Change)) on the abscissa and statistical significance expressed as -log(*p*-value) on the ordinate. Protein groups demonstrating statistically significant differences based on the Student's *t*-test are highlighted in red. The color version of the figure is available in the electronic version of the article.

apoptosis, GLIPR2, an autophagy suppressor, ubiquitin-containing proteins, and the antioxidant protein TXN. The most significant increase in expression was observed for hemostasis regulators (platelet glycoprotein GP6, protein disulfide isomerase PDIA5), platelet immunomodulators (CD226, LYN), intracellular trafficking regulators (EHD3, beta-amyloid precursor protein APP), and energy metabolism regulators (peptidylprolyl isomerase PPIF, FHL1).

Cluster Analysis and Functional Annotation of Protein Groups

Cluster analysis was performed using 499 proteins with significantly altered expression in at least one pairwise comparison by ANOVA with post-hoc analysis (q-value <0.05). Proteins were grouped into 20 clusters on a heatmap based on expression similarity using the k-means method (Fig. 3). Functional annotation using Fisher's exact method

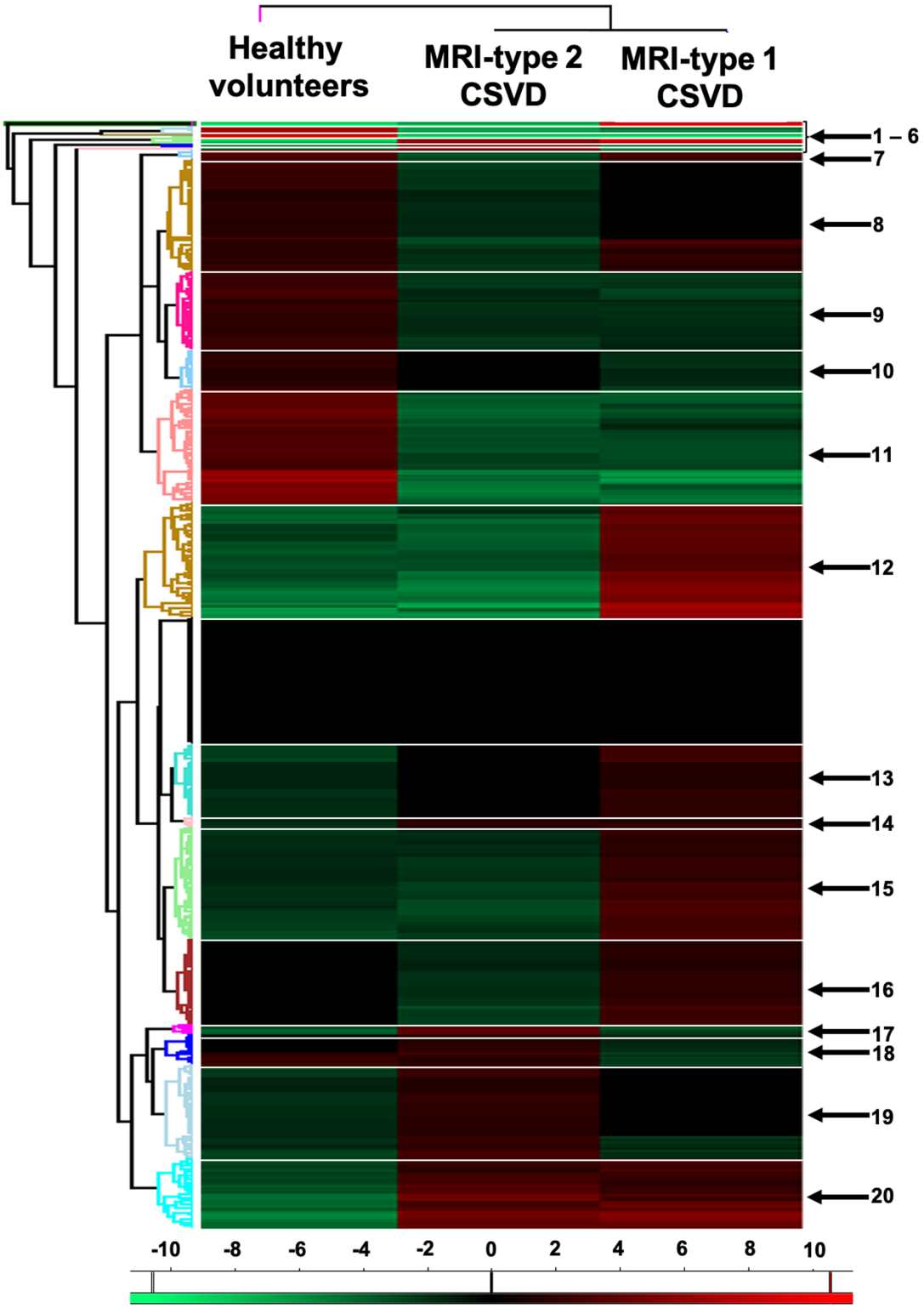

Figure 3. Heat map showing differences in the analysis of differentially expressed proteins in an ANOVA analysis for three groups. Cluster *1*, number of protein groups 2: hot pink. Cluster *2*, number of protein groups 4: pastel blue. Cluster *3*, number of protein groups 1: marsh. Cluster *4*, number of protein groups 3: light green. Cluster *5*, number of protein groups 2: dark blue. Cluster *6*, number of protein groups 1: pink. Cluster *7*, number of protein groups 4: sky-blue-1. Cluster *8*, number of protein groups 51: gold. Cluster *9*, number of protein groups 35: fuchsia-1. Cluster *10*, number of protein groups 18: sky-blue-2. Cluster *11*, number of protein groups 51: peach. Cluster *12*, number of protein groups 52: dark gold. Cluster *13*, number of protein groups 33: sea green. Cluster *14*, number of protein groups 5: light pink. Cluster *15*, number of protein groups 50: light green. Cluster *16*, number of protein groups 39: brown. Cluster *17*, number of protein groups 4: fuchsia-2. Cluster *18*, number of protein groups 14: blue. Cluster 19, number of protein groups 42: light blue. Cluster *20*, number of protein groups 32: bright blue.

revealed significant enrichment of molecular pathways from international databases for 9 clusters (clusters 7, 9, 10, 11, 12, 15, 16, 19, 20) (Fig. 3; Supplementary Material, Table S4).

Both cohorts of CSVD patients were characterized by a decrease in the expression of proteins from two large clusters, as compared to healthy volunteers: cluster 9 (35 proteins), functionally annotated to neutrophil degranulation and cluster 11 (51 proteins), associated with innate immunity, lysosome activation, ECM components, vesicular transport, and spatial modification of proteins. Cluster 11 is also annotated to the profile of genes with reduced expression in brain tissue in Alzheimer's disease. In CSVD patients the most pronounced decrease versus control group was found in case of the expression of RNase A from cluster 3 (RNAseA) and 4 proteins from cluster 2 (SORL1, TIMP2, PLAUR, PRG3), involved in neuroinflammation and interaction with the ECM. Moreover, for both CSVD MRI types, there was an increase (versus control group) in the expression of 32 proteins of cluster 20, involved in the regulation of the complement protein cascade and the acquired humoral immune response, as well as an increase in expression of three proteins of cluster 4 (SYTL4, IGJ, FGA), involved in the regulation of the humoral immune response and hemostasis. An increase in the expression of five proteins of cluster 14 (SNCA, PPIA, IGHA1, PRMT5, a group of actin proteins) is associated with an increase in the expression of proteins from the large unannotated cluster 13 (33 proteins); in patients with CSVD MRI type 1, this cluster is expressed more actively than in patients with CSVD MRI type 2, (versus control group). According to the STRING database, proteins of these two clusters are involved in stress-induced interactions of the actin cytoskeleton and vesicular transport of the cell with the external environment, primarily through the key hub protein, profillin-1.

The most generalized changes in protein expression profiles are observed in the cohort of patients with CSVD MRI type 1 compared to patients with CSVD MRI type 2 and healthy volunteers. The most pronounced increase in the expression of two proteins of cluster 1 (FGB, TPM4) is complemented by increased expression of proteins of clusters 12 (52 proteins), 15 (50 proteins), and 16 (39 proteins): they all are involved in the organization of intercellular contacts, platelet activation, and degranulation. Patients with MRI type 1 also show a more pronounced (than in patients with MRI type 2) decrease in the expression of 18 proteins of cluster 10 versus control group. These proteins are involved in ubiquitin-proteasome protein degradation, regulation of energy metabolism and the cell cycle, and apoptosis.

In patients with CSVD MRI type 2, changes in the protein expression profile were also detected versus patients with CSVD MRI type 2 and healthy volunteers; the most increased expression was noted for two proteins of cluster 5 (complement protein CFH and vasomodulatory protein arginase-1) and the ubiquitin-containing protein group of proteins of cluster 6 (RPS27A, UBC, UBB, UBA52). Increased expression of cluster 19 proteins (42 proteins) involved in the functioning of the ankyrin-1 complex and 4 proteins of cluster 17 (Ras proteins Ral-A and Rab-5B, immunoglobulin proteins IGLV3-10 and IGHV5-51) involved in the adaptive humoral immune response is associated with a marked increase in the expression of 14 proteins of the unannotated cluster 18, especially relative to the cohort of patients with MRI type 1. In the STRING database, proteins from these three associated clusters form a single network of protein-protein interactions indicating the regulation of energy metabolism and antioxidant protection of cells, vesicular transport, chromatin organization, immunity and inflammation, and cell adhesion. The key nodal proteins of the network are the glycolytic enzyme glyceraldehyde-3-phosphate dehydrogenase (GAPDH) and TXN. In patients with CSVD type 2 a decrease in the expression of four proteins of cluster 7 (DLD, HIST2H3A, HIST1H3A, SERPINA1) and 51 proteins of the unannotated cluster 8 was also observed compared to the group of patients with CSVD type 1 and healthy volunteers. According to the STRING database, these proteins form an interaction network associated with proinflammatory leukocyte differentiation, in particular, with mitochondrial and ER stress, glycoprotein synthesis, and lysosome maturation, which influence the expression of immune cell receptors and proinflammatory transcription factors (such as NF-κB). The key hub proteins in the interaction network are superoxide dismutase-2 (SOD2), heat shock protein HSP90AA1, and lysosomal protein LAMP1.

DISCUSSION

We conducted the first shotgun proteome study of peripheral blood samples from patients with various MRI types of CSVD. The results highlight several key aspects of sample preparation that affect the quality of the data obtained. Specifically, before washing the leukocyte fraction with cold PBS, the sediment must be thoroughly cleared of red blood cells by using erythrocyte lysis buffer. An equally important aspect is minimizing noise associated with stress factors during sample preparation (rapid temperature changes, aggressive cell suspension, and centrifugation).

The classical method of shotgun proteomics that we used can be improved. The use of data-independent acquisition (DIA) MS and cell deconvolution software

will enable more informative protein profiles to be obtained and assessed with correction for the ratio of different cell populations. The implementation of machine learning for the quantitative and spatial evaluation of CSVD MR features that meet the STRIVE criteria will improve the reliability and reproducibility of correlation analysis data for protein expression profiling.

Our differential expression analysis and cluster analysis of protein expression with functional annotation revealed a number of molecular genetic alterations that require further validation on larger sets of samples.

In particular, in patients with advanced stages of CSVD, a general trend towards decreased expression of a group of proteins associated with vesicular trafficking and ECM remodeling (including in the vascular endothelial basement membrane) was observed. These included the lysosomal enzymes GALNS [40, 41] and ARSA [42, 43], the metalloproteinase inhibitor TIMP2 [44], and the glycoprotein LRG1 [45]. Interestingly, this group of proteins has also been functionally annotated in relation to Alzheimer's disease; this is consistent with the current trend towards an increasing proportion of CSVD cases combined with neurodegeneration [15]. In particular, in CSVD patients we found a trend towards decreased expression of the transmembrane receptor SORL1. It carries out vesicular trafficking of the beta-amyloid precursor and its metabolic products; a decrease in its expression was detected in the brain tissue of patients with Alzheimer's disease [46].

It is known that the most common hereditary form of CSVD, cerebral autosomal dominant arteriopathy with subcortical infarcts and leukoencephalopathy (CADASIL), is also associated with the accumulation of glycoprotein granular osmophilic inclusions in the wall of small cerebral vessels [47]. Other hereditary forms of CSVD are associated with mutations in genes encoding lysosomal enzymes (CTSA) [48], components of the endothelial basement membrane ECM (COL4A1/COL4A2) [49]. Population genetic studies of sporadic forms of CSVD also confirm the association of CSVD with the expression of genes regulating the composition of the ECM (taking into account mathematical correction for vascular risk factors) [19]. In-depth study of the structure of the basement membrane, the ECM of the vascular wall, and the perivascular ECM of cerebral small vessels is necessary.

The low power of the patient samples with different MRI types of CSVD does not allow us to talk about significant differences in protein expression between these two groups. However, the results of a pilot study indicate a tendency towards insufficient activation of protective stress-induced proteins in patients with CSVD MRI type 1, characterized by an earlier age of onset and a more severe spectrum of clinical manifestations [35], as compared with CSVD MRI type 2. In particular, insufficient expression of arginase-1 and antioxidant proteins (TXN, etc.) can lead to NO-mediated damage to the BBB by reactive oxygen species and proinflammatory immune cells. In this context, suppression of Ras proteins, ubiquitin-containing proteins and autophagy suppressors can contribute to apoptosis of NVU components. Also, in the case of CSVD MRI type 1, it is necessary to confirm in future studies the tendency towards more intense activation of platelet proteins that increase the risk of microthrombosis, and proteins involved in stress-induced reorganization of the actin cytoskeleton and remodeling of the vascular wall (such as profilin-1) [50–52].

CONCLUSIONS

Our shotgun proteomic study has several significant limitations: a minimal sample size, contamination of some samples with non-target blood components, and the lack of cellular deconvolution during MS data analysis. However, the study results highlight the need for further study of protein expression profiles in the peripheral blood and cerebrospinal fluid of patients with various MRI types of CSVD by using larger sets of samples, including comparisons with RNA sequencing and immunohistochemical analysis results. This will deepen our understanding of the pathogenetic mechanisms of CSVD development and validate our approach to subdividing advanced CSVD stages into MRI types. Considering the etiopathogenetic heterogeneity of MRI manifestations of CSVD will improve the efficiency of the search for diagnostic biomarkers of the disease and candidate targets for targeted therapy.

ACKNOWLEDGEMENTS

The proteomic study, including sample preparation and MS measurements, was performed using the equipment of “Human Proteome” Core Facilities of the Institute of Biomedical Chemistry (Russia).

FUNDING

The proteomic analysis was conducted as part of the research project “The Effect of Compounds with Geroprotective Properties on Single Biomacromolecules, Model Objects, and the Human Body” with financial support from the Ministry of Science and Higher Education of the Russian Federation (Agreement no. 075-15-2024-643).

COMPLIANCE WITH ETHICAL STANDARDS

The blood plasma samples used in this study were initially obtained in compliance with all required ethical standards. All subjects signed informed consent to participate in the study and were informed about the subsequent use of their biological materials. The study was approved by the relevant Ethics Committee of the Russian Center for Neurology and Neuroscience (Protocol no. 3-3/24 dated April 15, 2024).

CONFLICT OF INTEREST

The authors declare no conflicts of interest.

Supplementary materials are available in the electronic version at the journal site (pbmc.ibmc.msk.ru).

REFERENCES

1. *Gorelick P.B., Scuteri A., Black S.E., DeCarli C., Greenberg S.M., Iadecola C., Launer L.J., Laurent S., Lopez O.L., Nyenhuis D., Petersen R.C., Schneider J.A., Tzourio C., Arnett D.K., Bennett D.A., Chui H.C., Higashida R.T., Lindquist R., Nilsson P.M., Roman G.C., Sellke F.W., Seshadri S.* (2011) Vascular contributions to cognitive impairment and dementia: a statement for healthcare professionals from the American Heart Association / American Stroke Association. Stroke, **42**(9), 2672–2713. DOI: 10.1161/STR.0b013e3182299496
2. *Wardlaw J.M., Smith E.E., Biessels G.J., Cordonnier C., Fazekas F., Frayne R., Lindley R.I., O'Brien J.T., Barkhof F., Benavente O.R., Black S.E., Brayne C., Breteler M., Chabriat H., DeCarli C., de Leeuw F.-E., Doubal F., Duering M., Fox N.C., Greenberg S., Hachinski V., Kilimann I., Mok V., van Oostenbrugge R., Pantoni L., Speck O., Stephan B.C.M., Teipel S., Viswanathan A., Werring D., Chen C., Smith C., van Buchem M., Norrving B., Gorelick P.B., Dichgans M.* (2013) Neuroimaging standards for research into small vessel disease and its contribution to ageing and neurodegeneration. Lancet Neurol., **12**(8), 822–838. DOI: 10.1016/S1474-4422(13)70124-8
3. *Rosenberg G.A., Wallin A., Wardlaw J.M., Markus H.S., Montaner J., Wolfson L., Iadecola C., Zlokovic B.V., Joutel A., Dichgans M., Duering M., Schmidt R., Korczyn A.D., Grinberg L.T., Chui H.C., Hachinski V.* (2016) Consensus statement for diagnosis of subcortical small vessel disease. J. Cereb. Blood Flow Metab., **36**(1), 6–25. DOI: 10.1038/jcbfm.2015.172
4. *Cannistraro R.J., Badi M., Eidelman B.H., Dickson D.W., Middlebrooks E.H., Meschia J.F.* (2019) CNS small vessel disease: a clinical review. Neurology, **92**(24), 1146–1156. DOI: 10.1212/WNL.0000000000007654
5. *Azarpazhooh M.R., Avan A., Cipriano L.E., Munoz D.G., Sposato L.A., Hachinski V.* (2018) Concomitant vascular and neurodegenerative pathologies double the risk of dementia. Alzheimers Dement., **14**(2), 148–156. DOI: 10.1016/j.jalz.2017.07.755
6. *Santisteban M.M., Iadecola C.* (2018) Hypertension, dietary salt and cognitive impairment. J. Cereb. Blood Flow Metab., **38**(12), 2112–2128. DOI: 10.1177/0271678X18803374
7. *Fisher C.M.* (1965) Lacunes: small, deep cerebral infarcts. Neurology, **15**(8), 774–784. DOI: 10.1212/wnl.15.8.774
8. *Fisher C.M.* (1982) Lacunar strokes and infarcts: a review. Neurology, **32**(8), 871–876. DOI: 10.1212/wnl.32.8.871
9. *Pantoni L.* (2010) Cerebral small vessel disease: from pathogenesis and clinical characteristics to therapeutic challenges. Lancet Neurol., **9**(7), 689–701. DOI: 10.1016/S1474-4422(10)70104-6
10. *Wardlaw J.M., Benveniste H., Williams A.* (2022) Cerebral vascular dysfunctions detected in human small vessel disease and implications for preclinical studies. Annu. Rev. Physiol., **84**, 409–434. DOI: 10.1146/annurev-physiol-060821-014521
11. *Markus H.S., de Leeuw F.E.* (2023) Cerebral small vessel disease: recent advances and future directions. Int. J. Stroke, **18**(1), 4–14. DOI: 10.1177/17474930221144911
12. *Williamson J.D., Pajewski N.M., Auchus A.P., Bryan R.N., Chelune G., Cheung A.K., Cleveland M.L., Coker L.H., Crowe M.G., Cushman W.C., Cutler J.A., Davatzikos C., Desiderio L., Erus G., Fine L.J., Gaussoin S.A., Harris D., Hsieh M.-K., Johnson K.C., Kimmel P.L., Tamura M.K., Launer L.J., Lerner A.J., Lewis C.E., Martindale-Adams J., Moy C.S., Nasrallah I.M., Nichols L.O., Oparil S., Ogrocki P.K., Rahman M., Rapp S.R., Reboussin D.M., Rocco M.V., Sachs B.C., Sink K.M., Still C.H., Supiano M.A., Snyder J.K., Wadley V.G., Walker J., Weiner D.E., Whelton P.K., Wilson V.M., Woolard N., Wright J.T. Jr., Wright C.B.; SPRINT MIND Investigators for the SPRINT Research Group* (2019) Effect of intensive vs standard blood pressure control on probable dementia: a randomized clinical trial. JAMA, **321**(6), 553–561. DOI: 10.1001/jama.2018.21442
13. *Hainsworth A.H., Markus H.S., Schneider J.A.* (2024) Cerebral small vessel disease, hypertension, and vascular contributions to cognitive impairment and dementia. Hypertension, **81**(1), 75–86. DOI: 10.1161/HYPERTENSIONAHA.123.19943
14. *Sonnen J.A., Santa Cruz K., Hemmy L.S., Woltjer R., Leverenz J.B., Montine K.S., Jack C.R., Kaye J., Lim K., Larson E.B., White L., Montine T.J.* (2011) Ecology of the aging human brain. Arch. Neurol., **68**(8), 1049–1056. DOI: 10.1001/archneurol.2011.157
15. *Toledo J.B., Arnold S.E., Raible K., Brettschneider J., Xie S.X., Grossman M., Monsell S.E., Kukull W.A., Trojanowski J.Q.* (2013) Contribution of cerebrovascular disease in autopsy confirmed neurodegenerative disease cases in the National Alzheimer's Coordinating Centre. Brain, **136**(Pt 9), 2697–2706. DOI: 10.1093/brain/awt188
16. *Kapasi A., Yu L., Petyuk V., Arfanakis K., Bennett D.A., Schneider J.A.* (2022) Association of small vessel disease with tau pathology. Acta Neuropathol., **143**(3), 349–362. DOI: 10.1007/s00401-021-02397-x
17. *Lammie G.A., Brannan F., Slattery J., Warlow C.* (1997) Nonhypertensive cerebral small-vessel disease. An autopsy study. Stroke, **28**(11), 2222–2229. DOI: 10.1161/01.str.28.11.2222
18. *Debette S., Schilling S., Duperron M.-G., Larsson S.C., Markus H.S.* (2019) Clinical significance of magnetic resonance imaging markers of vascular brain injury: a systematic review and meta-analysis. JAMA Neurol., **76**(1), 81–94. DOI: 10.1001/jamaneurol.2018.3122
19. *Bhagat R., Marini S., Romero J.R.* (2023) Genetic considerations in cerebral small vessel diseases. Front. Neurol., **14**, 1080168. DOI: 10.3389/fneur.2023.1080168

20. *Manini A., Pantoni L.* (2023) Genetic causes of cerebral small vessel diseases: a practical guide for neurologists. Neurology, **100**(16), 766–783. DOI: 10.1212/WNL.0000000000201720
21. *Joutel A., Haddad I., Ratelade J., Nelson M.T.* (2016) Perturbations of the cerebrovascular matrisome: a convergent mechanism in small vessel disease of the brain? J. Cereb. Blood Flow Metab., **36**(1), 143–157. DOI: 10.1038/jcbfm.2015.62
22. *Mok V.C.T., Cai Y., Markus H.S.* (2024) Vascular cognitive impairment and dementia: mechanisms, treatment, and future directions. Int. J. Stroke, **19**(8), 838–856. DOI: 10.1177/17474930241279888
23. *Zlokovic B.V.* (2011) Neurovascular pathways to neurodegeneration in Alzheimer's disease and other disorders. Nat. Rev. Neurosci., **12**(12), 723–738. DOI: 10.1038/nrn3114
24. *Beishon L., Panerai R.B.* (2021) The neurovascular unit in dementia: an opinion on current research and future directions. Front. Aging Neurosci., **13**, 721937. DOI: 10.3389/fnagi.2021.721937
25. *Dupré N., Drieu A., Joutel A.* (2024) Pathophysiology of cerebral small vessel disease: a journey through recent discoveries. J. Clin. Invest., **134**(10), e176330. DOI: 10.1172/JCI172841
26. *Mitroi D.N., Tian M., Kawaguchi R., Lowry W.E., Carmichael S.T.* (2022) Single-nucleus transcriptome analysis reveals disease- and regeneration-associated endothelial cells in white matter vascular dementia. J. Cell. Mol. Med., **26**(11), 3183–3195. DOI: 10.1111/jcmm.17315
27. *Raina A., Zhao X., Grove M.L., Bressler J., Gottesman R.F., Guan W., Pankow J.S., Boerwinkle E., Mosley T.H., Fornage M.* (2017) Cerebral white matter hyperintensities on MRI and acceleration of epigenetic aging: the atherosclerosis risk in communities study. Clin. Epigenetics, **9**, 21. DOI: 10.1186/s13148-016-0302-6
28. *Yang Y., Knol M.J., Wang R., Mishra A., Liu D., Luciano M., Teumer A., Armstrong N., Bis J.C., Jhun M.A., Li S., Adams H.H.H., Aziz N.A., Bastin M.E., Bourgey M., Brody J.A., Frenzel S., Gottesman R.F., Hosten N., Hou L., Kardia S.L.R., Lohner V., Marquis P., Maniega S.M., Satizabal C.L., Sorond F.A., Valdés Hernández M.C., van Duijn C.M., Vernooij M.W., Wittfeld K., Yang Q., Zhao W., Boerwinkle E., Levy D., Deary I.J., Jiang J., Mather K.A., Mosley T.H., Psaty B.M., Sachdev P.S., Smith J.A., Sotoodehnia N., DeCarli C.S., Breteler M.M.B., Ikram M.A., Grabe H.J., Wardlaw J., Longstreth W.T., Launer L.J., Seshadri S., Debette S., Fornage M.* (2023) Epigenetic and integrative cross-omics analyses of cerebral white matter hyperintensities on MRI. Brain, **146**(2), 492–506. DOI: 10.1093/brain/awac290
29. *Deng Y.-T., You J., He Y., Zhang Y., Li H.-Y., Wu X.-R., Cheng J.-Y., Guo Y., Long Z.-W., Chen Y.-L., Li Z.-Y., Yang L., Zhang Y.-R., Chen S.-D., Ge Y.-J., Huang Y.-Y., Shi L.-M., Dong Q., Mao Y., Feng J.-F., Cheng W., Yu J.-T.* (2025) Atlas of the plasma proteome in health and disease in 53,026 adults. Cell, **188**(1), 253–271.e7. DOI: 10.1016/j.cell.2024.10.045
30. *Wang Y.-C., Zhu H.-H., He L.-C., Yao Y.-T., Zhang L., Xue X.-L., Li J.-Y., Zhang L., Song B., Shi C.-H., Li Y.-S., Gao Y., Yang J.-H., Xu Y.-M.* (2025) Proteome profiling of serum reveals pathological mechanisms and biomarker candidates for cerebral small vessel disease. Transl. Stroke Res., **16**(6), 1606–1620. DOI: 10.1007/s12975-025-01332-6
31. *Hristovska I., Kumar A., Binette A.P., van Westen D., Janelidze S., Stomrud E., Palmqvist S., Ossenkoppele R., Mattsson-Carlgren N., Vogel J.W., Hansson O.* (2023) Identification of distinct and shared biomarkers in cerebral small vessel disease (SVD) through proteomic profiling of cerebrospinal fluid. Alzheimers Dement., **19**(Suppl 24), e082927. DOI: 10.1002/alz.082927
32. *Armstrong N.J., Mather K.A., Sargurupremraj M., Knol M.J., Malik R., Satizabal C.L., Yanek L.R., Wen W., Gudnason V.G., Dueker N.D., Elliott L.T., Hofer E., Bis J., Jahanshad N., Li S., Logue M.A., Luciano M., Scholz M., Smith A.V., Trompet S., Vojinovic D., Xia R., Alfaro-Almagro F., Ames D., Amin N., Amouyel P., Beiser A.S., Brodaty H., Deary I.J., Fennema-Notestine C., Gampawar P.G., Gottesman R., Griffanti L., Jack C.R. Jr., Jenkinson M., Jiang J., Kral B.G., Kwok J.B, Lampe L., Liewald D., Maillard P., Marchini J., Bastin M.E., Mazoyer B., Pirpamer L., Romero J.R., Roshchupkin G.V., Schofield P.R., Schroeter M.L., Stott D.J., Thalamuthu A., Trollor J., Tzourio C., van der Grond J., Vernooij M.W., Witte V.A., Wright M.J., Yang Q., Morris Z., Siggurdsson S., Psaty B., Villringer A., Schmidt H., Haberg A.K., van Duijn C.M., Jukema J.W., Dichgans M., Sacco R.L., Wright C.B., Kremen W.S., Becker L.C., Thompson P.M., Mosley T.H., Wardlaw J.M., Ikram M.A., Adams H.H.H., Seshadri S., Sachdev P.S., Smith S.M., Launer L., Longstreth W., DeCarli C., Schmidt R., Fornage M., Debette S., Nyquist P.A.* (2020). Common genetic variation indicates separate causes for periventricular and deep white matter hyperintensities. Stroke, **51**(7), 2111–2121. DOI: 10.1161/STROKEAHA.119.027544
33. *Chung J., Marini S., Pera J., Norrving B., Jimenez-Conde J., Roquer J., Fernandez-Cadenas I., Tirschwell D.L., Selim M., Brown D.L., Silliman S.L., Worrall B.B., Meschia J.F., Demel S., Greenberg S.M., Slowik A., Lindgren A., Schmidt R., Traylor M., Sargurupremraj M., Tiedt S., Malik R., Debette S., Dichgans M., Langefeld C.D., Woo D., Rosand J., Anderson C.D.* (2019) Genome-wide association study of cerebral small vessel disease reveals established and novel loci. Brain, **142**(10), 3176–3189. DOI: 10.1093/brain/awz233
34. *Duperron M.-G., Knol M.J., le Grand Q., Evans T.E., Mishra A., Tsuchida A., Roshchupkin G., Konuma T., Trégouët D.-A., Romero J.R., Frenzel S., Luciano M., Hofer E., Bourgey M., Dueker N.D., Delgado P., Hilal S., Tankard R.M., Dubost F., Shin J., Saba Y., Armstrong N.J., Bordes C., Bastin M.E., Beiser A., Brodaty H., Bülow R., Carrera C., Chen C., Cheng C.-Y., Deary I.J., Gampawar P.G., Himali J.J., Jiang J., Kawaguchi T., Li S., Macalli M., Marquis P., Morris Z., Muñoz Maniega S., Miyamoto S., Okawa M., Paradise M., Parva P., Rundek T., Sargurupremraj M., Schilling S., Setoh K., Soukarieh O., Tabara Y., Teumer A., Thalamuthu A., Trollor J.N., Valdés Hernández M.C., Vernooij M.W., Völker U., Wittfeld K., Wong T.Y., Wright M.J., Zhang J., Zhao W., Zhu Y.-C., Schmidt H., Sachdev P.S., Wen W., Yoshida K., Joutel A., Satizabal C.L., Sacco R.L., Bourque G.; CHARGE consortium; Lathrop M., Paus T., Fernandez-Cadenas I., Yang Q., Mazoyer B., Boutinaud P., Okada Y., Grabe H.J., Mather K.A., Schmidt R., Joliot M., Ikram M.A., Matsuda F., Tzourio C., Wardlaw J.M., Seshadri S., Adams H.H.H., Debette S.* (2023) Genomics of perivascular space burden unravels early mechanisms of cerebral small vessel disease. Nat. Med., **29**(4), 950–962. DOI: 10.1038/s41591-023-02268-w
35. *Dobrynina L.A., Gnedovskaya E.V., Zabitova M.R., Kremneva E.I., Shabalina A.A., Makarova A.G., Tzipushtanova M.M., Filatov A.D., Kalashnikova L.A.,*

Krotenkova M.V. (2020) Clustering of diagnostic MRI signs of cerebral microangiopathy and its relationship with markers of inflammation and angiogenesis. S.S. Korsakov Journal of Neurology and Psychiatry, **120**(12–2), 22–31. DOI: 10.17116/jnevro202012012222

36. *Soloveva N.A., Novikova S.E., Farafonova T.E., Tikhonova O.V., Zgoda V.G., Archakov A.I.* (2024) Proteome of plasma extracellular vesicles as a source of colorectal cancer biomarkers. Biomeditsinskaya Khimiya, **70**(5), 356–363. DOI: 10.18097/PBMC20247005356
37. *Prianichnikov N., Koch H., Koch S., Lubeck M., Heilig R., Brehmer S., Fischer R., Cox J.* (2020) MaxQuant software for ion mobility enhanced shotgun proteomics. Mol. Cell. Proteomics, **19**(6), 1058–1069. DOI: 10.1074/mcp.TIR119.001720
38. *Tyanova S., Cox J.* (2018) Perseus: a bioinformatics platform for integrative analysis of proteomics data in cancer research. Methods Mol. Biol., **1711**, 133–148. DOI: 10.1007/978-1-4939-7493-1_7
39. *Szklarczyk D., Nastou K., Koutrouli M., Kirsch R., Mehryary F., Hachilif R., Hu D., Peluso M.E., Huang Q., Fang T., Doncheva N.T., Pyysalo S., Bork P., Jensen L.J., von Mering C.* (2025) The STRING database in 2025: protein networks with directionality of regulation. Nucleic Acids Res., **53**(D1), D730–D737. DOI: 10.1093/nar/gkae1113
40. *Wang R.Y., Rudser K.D., Dengel D.R., Evanoff N., Steinberger J., Movsesyan N., Garrett R., Christensen K., Boylan D., Braddock S.R., Shinawi M., Gan Q., Montaño A.M.* (2020) Abnormally increased carotid intima media-thickness and elasticity in patients with Morquio A disease. Orphanet J. Rare Dis., **15**, 73. DOI: 10.1186/s13023-020-1331-y
41. *Powell A.W., Taylor M.D., Burrow T.A., Hopkin R.J., Prada C.E., Jefferies J.L.* (2017) Widespread vasculopathy in a patient with Morquio A syndrome. Texas Heart Inst. J., **44**(6), 420–423. DOI: 10.14503/THIJ-16-6121
42. *Fujita K., Teramura N., Hattori S., Irie S., Mitsunaga-Nakatsubo K., Akimoto Y., Sakamoto N., Yamamoto T., Akasaka K.* (2010) Mammalian arylsulfatase A functions as a novel component of the extracellular matrix. Connect. Tissue Res., **51**(5), 388–396. DOI: 10.3109/03008200903537097
43. *Zarekiani P., Breur M., Wolf N.I., de Vries H.E., van der Knaap M.S., Bugiani M.* (2021) Pathology of the neurovascular unit in leukodystrophies. Acta Neuropathol. Commun., **9**, 103. DOI: 10.1186/s40478-021-01206-6
44. *Kim S.H., Cho Y.-R., Kim H.-J., Oh J.S., Ahn E.-K., Ko H.-J., Hwang B.J., Lee S.-J., Cho Y., Kim Y.K., Stetler-Stevenson W.G., Seo D.-W.* (2012) Antagonism of VEGF-A-induced increase in vascular permeability by an integrin α3β1-Shp-1-cAMP/PKA pathway. Blood, **120**(24), 4892–4902. DOI: 10.1182/blood-2012-05-428243
45. *Hoeh A.E., Chang J.-H., Mueller R.S., Basche M., Fantin A., Sepetis A., de Rossi G., Dritsoula A., Ali R.R., Turowski P., Moss S.E., Greenwood J.* (2025) LRG1 alters pericyte phenotype and compromises vascular maturation. Cells, **14**(8), 690. DOI: 10.3390/cells14080593
46. *Scherzer C.R., Offe K., Gearing M., Rees H.D., Fang G., Heilman C.J., Schaller C., Bujo H., Levey A.I., Lah J.J.* (2004) Loss of apolipoprotein E receptor LR11 in Alzheimer disease. Arch. Neurol., **61**(8), 1200–1205. DOI: 10.1001/archneur.61.8.1200
47. *Illarioshkin S.N., Abramycheva N.Yu., Kalashnikova L.A., Maximova M.Yu., Konovalov R.N., Stepanova M.S., Fedotova E.Yu.* (2013) Clinical and molecular genetic analysis of cerebral autosomal dominant arteriopathy with subcortical infarcts and leukoencephalopathy (CADASIL) in Russian families. Nevrologicheskii Zhurnal, **18**(4), 8–16.
48. *Bugiani M., Kevelam S.H., Bakels H.S., Waisfisz Q., Ceuterick-de Groote C., Niessen H.W.M., Abbink T.E.M., Lesnik Oberstein S.A.M.J., van der Knaap M.S.* (2016) Cathepsin A-related arteriopathy with strokes and leukoencephalopathy (CARASAL). Neurology, **87**(17), 1777–1786. DOI: 10.1212/WNL.0000000000003251
49. *Engel J., Prockop D.J.* (1991) The zipper-like folding of collagen triple helices and the effects of mutations that disrupt the zipper. Annu. Rev. Biophys. Biophys. Chem., **20**, 137–152. DOI: 10.1146/annurev.bb.20.060191.001033
50. *Caglayan E., Romeo G.R., Kappert K., Odenthal M., Südkamp M., Body S.C., Shernan S.K., Hackbusch D., Vantler M., Kazlauskas A., Rosenkranz S.* (2010) Profilin-1 is expressed in human atherosclerotic plaques and induces atherogenic effects on vascular smooth muscle cells. PLOS One, **5**(10), e13608. DOI: 10.1371/journal.pone.0013608
51. *Wang Y., Zhang J., Gao H., Zhao S., Ji X., Liu X., You B., Li X., Qiu J.* (2014) Profilin-1 promotes the development of hypertension-induced artery remodeling. J. Histochem. Cytochem., **62**(4), 298–310. DOI: 10.1369/0022155414520978
52. *Xie Q., Ma L., Xiao Z., Yang M., Chen M.* (2023) Role of profilin-1 in vasculopathy induced by advanced glycation end products (AGEs). J. Diabetes Complications, **37**(5), 108415. DOI: 10.1016/j.jdiacomp.2023.108415

Received: 16.12.2025.
Revised: 15.03.2026.
Accepted: 17.03.2026.

ПИЛОТНОЕ ПАНОРАМНОЕ ИССЛЕДОВАНИЕ ПРОТЕОМА МОНОНУКЛЕАРОВ ПЕРИФЕРИЧЕСКОЙ КРОВИ У ПАЦИЕНТОВ С РАЗЛИЧНЫМИ МРТ-ТИПАМИ ЦЕРЕБРАЛЬНОЙ МИКРОАНГИОПАТИИ

А.А. Гейнц[1]*, П.С. Шлапакова[1], Л.А. Добрынина[1], Е.И. Кремнева[1], Е.В. Хряпова[2], В.Г. Згода[2], О.В. Тихонова[2]

[1]Российский центр неврологии и нейронаук,
125367, Москва, Волоколамское шоссе, 80; *эл. почта: gejnts.a.a@neurology.ru
[2]Научно-исследовательский институт биомедицинской химии имени В.Н. Ореховича,
119121, Москва, ул. Погодинская, 10

Возраст-зависимая церебральная микроангиопатия (ЦМА), ассоциированная с сосудистыми факторами риска, является одной из основных причин когнитивных расстройств и инсультов. Сложности изучения ЦМА обусловлены ограничениями в визуализации мелких сосудов, диагностикой на основании МРТ-признаков поражения вещества головного мозга (гиперинтенсивность белого вещества, лакуны, микрокровоизлияния и др.). Проведённая нами ранее оценка каждого из МРТ-признака ЦМА по четырёхбалльной системе выраженности и распределению по отделам мозга при кластерном анализе установила существование двух МРТ-типов, не отличающихся по выраженности сосудистых факторов риска, но имеющих различия в тяжести клинических проявлений и уровне циркулирующих биомаркеров плазмы крови. В данной работе проведено пилотное панорамное исследование протеома мононуклеаров периферической крови для пациентов с первым и вторым МРТ-типами ЦМА, а также здоровых добровольцев. У пациентов с ЦМА выявлена тенденция к снижению уровня белков, ассоциированных с везикулярным трафиком и ремоделированию внеклеточного матрикса (ВКМ), относительно нормы. У пациентов с первым МРТ-типом ЦМА выявлены тенденции к недостаточной активации защитных белков (аргиназа-1, тиоредоксин, регуляторы аутофагии и белкового стресса), при чрезмерной активации тромбоцитарных белков и регуляторов ремоделирования сосудистой стенки (таких как профиллин-1), по сравнению со вторым МРТ-типом. Полученные результаты указывают на необходимость изучения микроструктуры базальной мембраны, ВКМ сосудистой стенки и периваскулярных пространств для церебральных мелких сосудов.

Полный текст статьи на русском языке доступен на сайте журнала (http://pbmc.ibmc.msk.ru).

Ключевые слова: церебральная микроангиопатия; болезнь мелких сосудов головного мозга; протеомные исследования; магнитно-резонансная томография; STRIVE-критерии; масс-спектрометрия белков

Финансирование. Протеомный анализ выполнен в рамках темы “Влияние соединений, обладающих геропротективными свойствами, на единичные биомакромолекулы, модельные объекты и организм человека” при финансовой поддержке Министерства науки и высшего образования Российской Федерации (Соглашение № 075-15-2024-643).

Поступила в редакцию: 16.12.2025; после доработки: 15.03.2026; принята к печати: 17.03.2026.